ChemComm

Accepted Manuscript

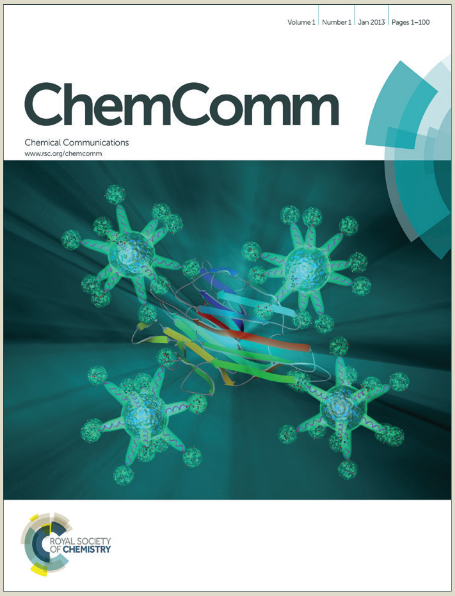

ROYAL SOCIETY OF CHEMISTRY

www.rsc.org/chemcomm

Journal Name

RSCPublishing

ARTICLE

Cite this: DOI: 10.1039/x0xx00000x

Self-assembled hierarchical yolk-shell structured NiO@C from metal-organic frameworks with outstanding performance for lithium storage

Lixiang Liu, Hong Guo*, Jiajia Liu, Fang Qian, Conghai Zhang, Tingting Li, Weiwei Chen, Xiangjun Yang* and Yicheng Guo

Received 00th January 2012,
Accepted 00th January 2012

DOI: 10.1039/x0xx00000x

www.rsc.org/

A facile generic environmental strategy is employed to prepare hierarchical yolk-shell hybrid NiO@C materials vis metal-organic frameworks. The intrinsic yolk-shell nature as well as the multi-elements characteristics of active components of the unique nanostructures contributes greatly to the outstanding electrochemical performance.

Precise control of the crystal structure, size, shape and chemical composition not only allows one to observe unique properties of the nano/micro-materials but can tune their fascinating properties of chemistry and physics as desired, and thus is one of the central tasks of modern science and technology.[1,2] Advanced materials with hollow structures have attracted much attention in a diverse range of applications such as drug delivery, environmental remediation, energy storage and various new applications, because of its well-defined interior voids, high specific surface area, low density, accommodate volume change without pulverizing compared with that of solid counterparts of the same size.[3-5] Especially, yolk-shell hybird micro/nano-structures exhibit considerable application in both fundamental research and practical applications due to their unique properties. For instance, TiO_2 based core/shell materials with different size and morphologies have enhanced photocatalytic and electrochemical properties.[6,7] Our previous prepared hollow cage-bell Ag@TiO_2 materials exhibit enhanced lithium-ion storage.[8] Lou and co-workers synthesized coaxial SnO_2@carbon hollow nanospheres for highly reversible lithium storage.[9] Therefore, a general approach to rationally fabricate yolk-shell hybrid structural materials is still lacking and it is desirable to obtain the materials through more facile, economic and environment-friendly process.

Metal–organic frameworks (MOFs), a new class of organic-inorganic hybrid functional materials with high porosity, large surface area and morphology can be easily tuned upon selection of different metal ions and organic bridging ligands.[10,11] Recently, MOFs have been proved to be an effective template for preparing hollow transition metal oxides by thermal decomposition, because the porosity and long-range ordering of MOFs can offer a fast and convenient access for incoming and leaving small molecules and ions in the transformation process.[11] In this MOFs templated solid-solid transformation process, noticeably, calcination conditions (e.g., temperature and atmosphere) significantly influence the structure and composition of as-obtained hollow products. For instance, Low et al. prepared Fe_2O_3 microboxes with hierarchically structured shells simply via annealing Prussian blue (PB) microcubes in air. Jaephil Cho et al. reported the spindle-like porous α-Fe_2O_3 prepared from a typical iron-based MOF template (MIL-88-Fe).[12] Though these methods are effective routes, they generally have some problems: difficulty in template fabrication, low product yields, and multisteps and costly operations. Besides, to our best knowledge, reports on the fast synthesis of yolk-shell structures derived from MOFs are quite rare.

Herein, we chose Ni-O-C to demonstrate our concept and propose a facile fast strategy to prepare yolk-shell structures from MOFs as Scheme 1.

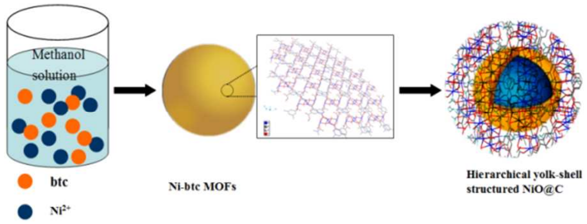

Scheme 1 Representative illustration of the formation of hierarchical yolk-shelll hybrid NiO@C.

NiO, a type of spinel transition metal oxide (TMO), has attracted considerable interest as high capacity anode materials for LIBs.[13-15] However, those electrodes suffer severe mechanical disintegration due to the drastic volumetric changes during lithium ion insertion and extraction, and therefore leads to rapid deterioration in capacity. In this work, the advantage of novel yolk-shell structures from MOFs and the virtue of hybrid matrix of distinct material systems are well integrated to solve the problem. Compared with conventional methods produced metal oxides nano electrodes,[16] the yolk-shell nanostructures prepared via MOFs have relatively high surface area and a stable hollow configuration without the destructive effect of template removal on product morphology. The hollow structures can render much contact area between active components and Li ions in the process of electrochemical reaction. Meanwhile, it may help the electrode to accommodate large volume change without pulverizing. Futhermore, the unique structure can shorten ionic/electronic diffusion length and provide efficient channels for mass transport.[17] The multi-components allow the electrochemical reaction to proceed in a hybrid matrix of distinct material systems.[18,19] In this case, the confining matrix may lead to the volume change occurs in a step-wise manner rather than at a certain fixed potential, thus the unreacted component can accommodate the strain yielded by the reacted phase. Futhermore, the coupling of carbon could render the TMOs with rich redox reactions and improve electronic conductivity.[20] As a result, the hierarchical NiO@C yolk-shell structures from metal-organic frameworks are anticipated to manifest outstanding electrochemical performance.

The whole fabrication process, experimental section, XRD (Fig.S1), FTIR spectrum (Fig. S2), and TG analysis (Fig. S3) of the hierarchical yolk-shell structured NiO@C are listed in ESI†. SEM images of the prepared Ni-MOF precursor and yolk-shell structured NiO@C yielded by calcinations at 450 °C and the molecular structures are shown as Fig. 1a-d. It is obvious that the Ni-MOF precursors are composed of solid microsphere particles. Close-up view (inset in Fig. 1a) reveals that these solid microspheres have a smooth surface. The structure of Ni-btc MOFs is shown as Fig. 1b. After calcining the Ni-MOF precursors at 450 °C for 2 h, a fluffy black powder is obtained and the typical morphology is presented in Fig. 1c, illuminating the products are uniform spherical shape ca.3 μm. It is interesting to find that the NiO@C mesosphere for Ni-MOFs is not a solid ball but a hollow core-shell structure, as evidenced by the partially broken shell vividly. The thickness of shell is estimated to ca. 30-50 nm and the surface of the synthesized NiO@C powder is made up of nano-sized small particles. The cleft of these particles might be caused by rapid mass-transport across the shells during calcinations. Fig. 1d is the molecular structure of NiO@C from Ni-MOFs. The unique hollow core-shell morphology of NiO@C nanoparticle aggregates is also characterized by TEM and HR-TEM, as illustrated in Fig. 1e and f. The TEM image in Fig. 1e shows a hollow core-void-shell microsphere, which is a visible hollow interior structure obviously. Especially, a typical structure with well-defined interior and very thin shell can also be detected and the thin thickness of shell of samples is ca. 40 nm, which is in good agreement with SEM analysis. Futhermore, the surface of samples exhibits a net frame, which hierarchical core-shell structure is resulted from MOFs. Its selected-area electron diffraction (SAED) pattern (Fig 1e inset) reveals the diffraction rings 1-3 are indexed to (1 1 1), (2 2 0), and (2 0 0) diffraction of face-centered cubic NiO, respectively. The lattice fringe is observed obviously, and the lattice spacing (0.244 nm) agrees with NiO (1 1 1) plane spacing from Fig. 1f.

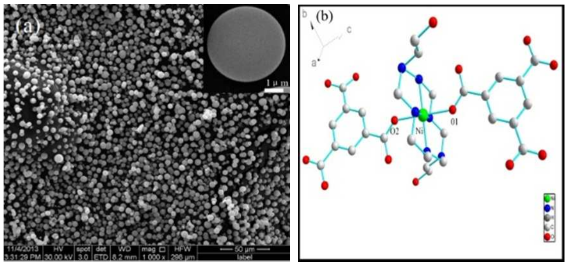

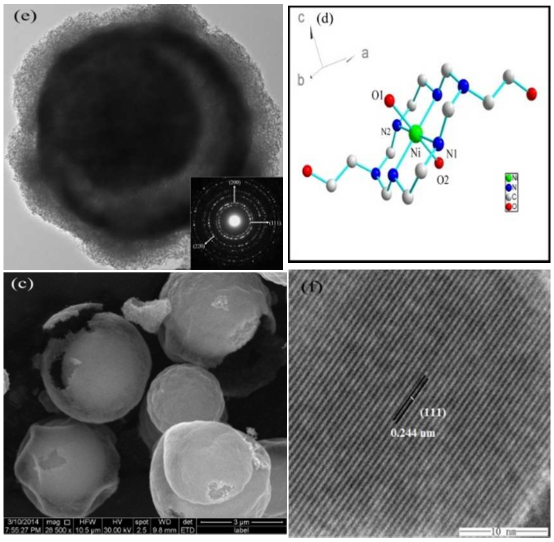

Fig. 1 SEM image (a) and the atomic space structure of Ni-btc MOFs precursor (b). SEM (c) , the residual atomic space structure (d), TEM (e) and HRTEM (f) micrographsthe of as-prepared yolk-shell NiO@C structures, which is yielded by solvothermal alcoholysis at 150 °C for 24 h and subsequent calcinations in air at 450 °C for 2 h. The inset in (e) is the selected area electron diffraction (SAED).

The BET surface area of the sample is 182.646 m^2 g^{-1} (seeing Fig. S4). Remarkably, the specific surface area of NiO is far higher than most of the previous reported NiO microsphere products. The formation mechanism are described as Fig. S5 in ESI†. The electrical conductivity of the obtained NiO-C products is 8.68×10^{-3} $\Omega^{-1}cm^{-1}$, which is much enhanced than NiO-GNS composite reported by Wang.[21] The electrochemical performance of the prepared yolk-shell NiO@C from MOFs used for Li-ion anodic materials is investigated. According to Fig. 2a, the increase in cycling stability and capacity with the increase of reaction time from 6 h to 24 h is mainly attributed to the formation of hierarchical yolk-shell structures. The capacity of the sample corresponding to 30 h can also remain stable as high as 960 $mAhg^{-1}$ after 200 cycles with a little lower than that of 24 h. However, when the reacted time arrived at 48 h, its capacity fades drastically from 1253 to 520 $mAhg^{-1}$ after 200 cycles. This result is understandable because the yolk-shell structures are destroyed in the process of alcoholysis reaction. The charge/discharge and cycle CV curves of hierarchical yolk-shell NiO@C (alcoholysis reaction time of 24 h) electrode are shown in Fig. 2b and c, respectively. According to the 1st, 2nd, and 200th discharge (Li^+ insertion) and charge (Li^+ extraction) curves at a current density of 1 C in the voltage window of 0.01-3 V. There is a wide, steady discharging plateau at 0.80 V in the first cycle, followed by a gradual voltage decrease. The initial discharge and charge capacities are 1292 and 955 $mAhg^{-1}$, respectively. The initial capacity loss is 26%, which should be attributed to the formation of solid electrolyte interphase (SEI) and the reduction of metal oxide to metal with Li_2O formation. The initial coulombic efficiency is 74%,[22] which is higher than most reported Ni-based oxide electrodes.[21,23] From the second cycle onwards, the long potential plateau was replaced by a long slope between 1.5 and 0.70 V. After 200 cycles, the capacity can also be kept at 962 $mAhg^{-1}$, showing the excellent reversibility of electrode. Cyclic voltammograms (CV) further reveal the lithium storage process of the NiO@C composites (Fig. 2c). In the cathodic process, the main reduction peak at 0.82 V and weak reduction peak at 1.31 V correspond to the reduction of

NiO to metallic Ni nanoparticles and the formation of a partially reversible SEI layer,[24,25] respectively. The oxidation peak at 1.51 V is associated with the partial decomposition of the SEI layer, and another oxidation peak at 2.42 V corresponds to the decomposition of Li_2O leading to the formation of NiO.[24,25] These results are consistent with charge-discarge analysis. To investigate electrochemistry performance under the different rate discharge, Fig. 2d exhibits the discharge capacities of NiO@C electrode against different current rates from 1 C to 20 C, and each sustained for 40 cycles. The stable cyclic performance is obtained for all rates. Even when the current reaches 20 C, the capacity can also arrive at 850 $mAhg^{-1}$. Subsequently, a specific capacity of ca. 940 $mAhg^{-1}$ is recovered when the current rate reduces back to 1 C after 200 cycles. The overall rate performance demonstrates the high capacities in both low and high current rates of the hierarchical yolk-shell NiO@C electrode.[26] Fig. 3 is the TEM of NiO@C electrode after 200 cycles at current density of 1 C, revealing materials is still kept well without breakage in the process of charge-discharge. Compared with the previous reported TMOs materials,[27,28] the material reported here is very attractive due to its facile, fast, and improved lithium storage. The nano-scaled characteristics of NiO particle from MOFs embedded in the aggregates ensure the electrode having a high capacity and the fast Li-ion diffusion in the electrode, and the introduction of carbon renders the electrode having a good electronic conductivity. The unique yolk-shell structures can shorten the length of Li-ion diffusion, which is benefit for the rate performance. The hollow structure offers a sufficient void space, which sufficiently alleviates the mechanical stress caused by volume change.[29] The multi-elements characteristics allow the volume change to take place in a stepwise manner during electrochemical cycle. Therefore, the hierarchical yolk-shell NiO@C electrode exhibits excellent electrochemical performance.

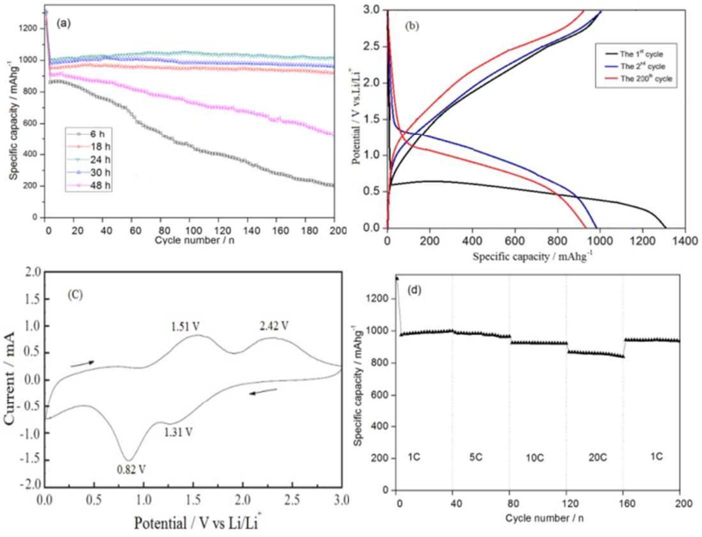

Fig. 2 Electrochemical performance of prepared yolk-shell structured NiO@C electrode: (a) cycling performance of NiO materials with different solvothermal alcoholysis time from 2 h to 48 h at constant current density of 1 C. (b) charge/discharge curves of NiO (alcoholysis reaction time of 24 h) electrode for the 1st, 2nd, and 200th cycle at current density of 1 C. (c) the first cycle CV curve with a scan rate of 0.05 mVs^{-1}. (d) rate capability of NiO electrode from 1 C to 20 C for 200 cycles. Electrode potential range of 0.01-3.0 V vs. Li/Li^+.

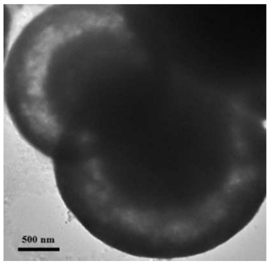

Fig. 3 TEM image of hybrid yolk-shell structured NiO@C electrodes after 200 cycles at 1C.

In summary, hierarchical yolk-shell structured NiO@C electrodes from MOFs are successfully synthesized by a facile and fast benign procedure via alcoholysis synthesis reaction. The stable reversible capacity of electrode can be retained at 962 $mAhg^{-1}$ after 200 cycles, and it also exhibit excellent rate performance. This strategy is simple, cheap and mass-productive, which may shed light on a new avenue for fast synthesis of yolk-shell structural nano/micro-functional materials derived from MOFs for energy storage, sensor, catalyst, and other new applications.

The authors would like to acknowledge financial support provided by Major state basic research development program of China (973 Program, No. 2014CB643406).

Notes and references

School of Chemistry Science and Engineering, Yunnan University, Kunming 650091,Yunnan, China. Fax: +86-871-65036626; Tel: +86-871-65032180; E-mail: guohongcom@126.com (Hong Guo), yxjun@ynu.edu.cn (Xiangjun Yang)

Electronic Supplementary Information (ESI) available: [details of any supplementary information available should be included here]. See DOI: 10.1039/b000000x/

1 J. Liu, S. Z. Qiao, S. B. Hartono and G. Q. M. Lu, *Angew. Chem.* 2010, **122**, 5101.
2 B. Wang, J. S. Chen, H. B. Wu, Z. Y. Wang and X. W. Lou, *J. Am. Chem. Soc.* 2011, **133**, 17146.
3 H. Guo, D. Tian, L. Liu, Y. Wang, Y. Guo and X. Yang, *J. Solid State Chem*., 2013, **201**, 137.
4 Y. Yin, R. M. Rioux, C. K. Erdonmez, S. Hughes, S, G. A. Somorjai and A. P. Alivisatos, *Science.* 2004, **304**, 711
5 L. Liu, Y. Guo, Y. Peng, X. Yang, S. Wang and H. Guo, *Electrochim. Acta*, 2013, **114**, 42.
6 H. Guo, Y.P. Wang, W. Wang, L.X. Liu, Y.Y. Guo, X.J. Yang, S.X. *Wang, Part. Part. Syst. Charact*. 2014, **31**,374.
7 X. Lai, J. Li, B.A. Korgel, Z. Dong, Z. Li, F. Su, J. Du, D. Wang, *Angew. Chem. Int. Ed*., 2011, **50**, 2738.
8 H. Guo, W. Wang, L. Liu, Y. He, C. Li, Y. Wang. *Green Chem.* 2013, **15**, 2810.
9 L. Zhou, D. Zhao, X. W. Lou, *Adv. Mater.,* 2012, **24**, 745.
10 J. Sculley, D. Q. Yuan and H. C. Zhou, *Energy Environ. Sci*., 2011, **4**, 2721.
11 L. E. Lauren, K. Leong, O. K. Farha, M. Allendorf, R. P. V. Duyne and J. T. Hupp, *Chem. Rev*., 2012, **112**, 1105.
12 X. D. Xu, R. G. Cao, S. Jeong, J. Cho, *Nano Lett.* 2012, **12**, 4988.
13 F. Y. Cheng, H. B. Wang, Z. Q. Zhu, Y. Wang, T. R. Zhang, Z. L. Tao, J. Chen, *Energy Environ. Sci*., 2011, **4**, 3668.
14 F. M. Courtel, H. Duncan, Y. Abu-Lebdeh, I. J.Davidson, J. *Mater. Chem*., 2011, **21**, 10206.
15 Y. Xia, W.K. Zhang, Z. Xiao, H. Huang, H.J. Zeng, X.R. Chen, F. Chen, Y.P. Gan, X.Y. Tao, *J. Mater. Chem.* 2012, **22**, 9209.
16 H. Guo, W. Wang, L. Liu, Y. He, C. Li, Y. Wang, *Green Chem*., 2013, **15**, 2810.
17 Z. Y. Wang, L. Zhou and X. W. Lou, *Adv. Mater.*, 2012, **24**, 1903.
18 H. Guo, L. Liu, T. Li, W. Chen, Y. Wang, W. Wang, *Chem. Commun.,* 2014, 50, 673.
19 I.R.M. Kottegoda, N.H. Idris, L. Lu, J.Z. Wang, H.K. Liu, *Electrochim. Acta*, 2011, **56**, 5815.

20 M. Hassan, M. Rahman, Z. Guo, Z. Chen, H. Liu, *J. Mater. Chem.*, 2010,**20**, 9707.
21 Y. Zou, Y. Wang, *Nanoscale,* 2011, **3**, 2615.
22 X. Huang, J. Tu, C. Zhang, J. Xiang, *Electrochem. Commun*., 2007, **9**, 1180.
23 P. R. Griffiths and D.J.A. Haseth, Fourier Transform Infrared Spectrometry*, John Wilely & Sons, New York,* **1986**.
24 Y.F. Yuan, X.H. Xia, J.B. Wu, J.L. Yang, Y.B. Chen, S.Y. Guo, *Electrochem. Commun.*, 2010, **12**, 890.
25 X.H. Wang, Z.B. Yang, X.L. Sun, X.W. Li, D.S. Wang, P. Wang and D.Y. He, *J. Mater. Chem*., 2011, **21**, 9988.
26 F. Chen, W. Zhou, H. Yao, P. Fan, J. Yang, Z. Fei, M. Zhong, *Green Chem.*, 2013,**15**, 3057.
27 G. Q. Zhang, H. B. Wu, H. E. Hoster, M. B. Chan-Park and X. W. Lou, *Energy Environ*. Sci., 2012, **5**, 9453.
28 H. Jiang, J. Ma and C. Z. Li, *Chem. Commun.*, 2012, **48**, 4465.
29 H. Guo, L. Liu, T. Li, W. Wang, W. Chen, J. Liu, Y. Guo, *Nanoscale,* 2014, **6**, 5491.